RSC Advances

ROYAL SOCIETY OF CHEMISTRY

www.rsc.org/advances

Accelerated co-precipitation of lead, zinc and copper by carbon dioxide bubbling in alkaline Municipal solid waste incinerator (MSWI) fly ash wash water

L. Wang[1, 2] *, Q. Chen[1], I.A. Jamro[1] , R.D. Li[1], H.A Baloch[1]

[1] *College of Energy and Environment, Shenyang Aerospace University, Shenyang 110036, China*

[2] *Chemical and Biological Engineering, the University of British Columbia, Vancouver V6T 1Z4, Canada*

Abstract: MSWI fly ash is a potential substitute for some virgin materials, but the soluble salts and hazardous trace elements in the ash can limit this potential. This study investigated the use of a water-based washing process to remove the soluble salts from MSWI fly ash. The removal of trace elements by bubbling CO_2 through the resulting wastewater was also evaluated and compared to the use of Na_2CO_3 solution. Washing was accomplished at liquid-to-solid ratios (L/S) (L/kg) ranging from 3 to 20, and at durations from 5 min to 1 h. The optimum washing condition was indentified by orthogonal test and the L/S ratio of 10 for 10 min. The extraction of chlorides by washing ranged from 62% to 95%, while the extraction of sulfate was less than 50% because the solubility of these salts was strongly influenced by the L/S ratio. Critical trace elements (lead, Zinc and copper) were also leached in high concentrations (63.7 $mg \cdot L^{-1}$, 4.53 $mg \cdot L^{-1}$ and 0.40 $mg \cdot L^{-1}$, respectively) at the optimum washing condition. These elements were effectively removed in the $CaCO_3$ or ferrum/aluminum-hydroxides that precipitated when CO_2 was bubbled into the wastewater. Various analyses showed that the precipitate was primarily $CaCO_3$ that formed into spheres. The concentration of trace elements incorporated into the precipitate varied across the radius of the sphere. A geochemical model was used to help explain the mechanism of trace elements precipitation. The accelerated carbonation of the alkaline MSWI fly ash washes water was effective in removing trace elements (Pb, Zn and Cu).

Keywords: MSWI fly ash; trace element; washing process; co-precipitation; PHREEQC

*Corresponding author. Tel.: +86 24 8972 3734; fax: +86 24 8972 4558.
E-mail address: wlei05@mails.tsinghua.edu.cn

1. Introduction

Waste reduction and reuse is a key requirement for a sustainable society. Incineration is commonly used to manage municipal solid wastes, primarily for volume reduction.[1] Unfortunately, municipal solid waste incinerator (MSWI) fly ash is usually classified as a hazardous waste because it contains toxic elements, soluble salts and organic compounds.[2] Yet, MSWI ash may be a valuable resource because of its other components and its silicate characteristics.[3] Numerous studies have examined replacing a portion of the raw materials used to produce cement with MSWI fly ash.[4-9] However, soluble salts, especially those of chlorine, have a strong influence on the partitioning of many toxic metals between their vapor and condensed phases, and have thus hindered the use of MSWI fly ash in the production of cement or clinkers.[10, 11] The water washing process is the most easily conducted and economical method of removing chloride from fly ash.[12-14] Kirby and Rimstidt[15] found that the ash-water solutions resulting from MSWI ash washing are dominated by ions released by soluble salts, and that these salts dissolve completely within minutes. Wang et al. [16] used a wide range of liquid-to-solid (L/S) ratios ranging from 2 to 100 in the washing process and found that more than 65% of the chloride element (Cl), and more than 50% of the major elements of sodium (Na), potassium (K), and calcium (Ca), as well as more than 30% of the chromium (Cr), were found to be leachable at L/S = 2. Chimenos et al. [14]focused on minimizing water consumption and reaction time in removing the maximum amount of chloride and heavy metals, and found the best combination of water use and washing duration was an L/S = 2 for 1 h. Other researchers found that a triple extraction of fly ash with water at L/S = 2 for 5 min gave the best results for removing Ca^{2+}, Na^{+}, K^{+}, chloride ion (Cl^{-}) and sulfate ion (SO_4^{2-}). [13]The variation in these results is due to different characteristics of samples, such as fly ash or bottom ash, and to experimental conditions.

Washing to remove soluble salts also extracts critical trace elements in high concentrations, and therefore produces a highly contaminated wastewater. Some researchers have investigated the immobilization of trace elements in wastewater using chemical reagents.[11, 17] Mangialardi[11] found that wastewater treatment can be successfully realized by simply reducing pH to values of 6.5–7.5 through addition of concentrated hydrochloric acid, followed by agitation. He also used an anionic, polyamide-type polyelectrolyte at a dosage of 2 mg L^{-1} to enhance the flocculation of solid particles.

This treatment was capable of removing various contaminants (aluminum (Al), cadium (Cd), lead (Pb), and zinc (Zn) ions) through two different mechanisms: precipitation of aluminum ions as metallic hydroxides, and adsorption of Cd, Pb, and Zn ions onto floc particles of aluminum hydroxide.

Currently, greenhouse gases (mainly carbon dioxide, CO_2) are a global issue. The recent interest in developing geochemical engineering methods to sequester, or at least retard, the migration of CO_2 has created a convincing need to understand the reactions between CO_2 and alkaline materials and minerals. In addition, the reuse of wastes that contain alkaline materials (such as MSWI fly ash and waste steel slag) is gaining in popularity.[18]

Wastewater from the washing of MSWI fly ash typically contains a high concentration of the Ca^{2+} ion, which is effective in sequestering CO_2. Likewise, waste industrial gases (such as cement kiln tail gas and power plant tail gas) are abundant in CO_2 and can be used to neutralize a variety of alkaline wastes. Thus, bubbling industrial tail gas into wastewater from fly ash washing would seem to offer several advantages: 1) the gas can neutralize the wastewater; 2) the wastewater can sequester the carbon dioxide in the gas; 3) reaction products can sequester the trace elements in the wastewater by incorporating them into calcite or adsorption on ferrum (Fe)/Al colloids; and 4) simultaneous reuse of the two "wastes" is economical and free from environmental risks. Further, compared with simpler acid neutralization, CO_2 bubbling 1) is not as aggressive as hydrochloric acid, sulfuric acid or other strong acid and 2) enhances the precipitation of selected trace elements because of the co-precipitation with calcium carbonate ($CaCO_3$).

In this paper, we report our research into washing of MSWI fly ash and how CO_2 and sodium carbonate (Na_2CO_3) solution react with the resulting MSWI fly ash wastewater to affect the precipitation behavior of various trace elements in the wastewater. We also studied how these two chemical agents neutralized the highly alkaline wastewater. The precipitation behavior of trace elements was modeled by PHREEQC (2.15), a geochemical code.

2. Materials and methods

2.1 Materials

The fly ash used in this study was obtained from an MSWI facility located in Mudu of Suzhou, China. The plant began to operate in 2006 with a capacity of 1000 $t \cdot d^{-1}$ and produces electrical power (12,000 KWh). The plant uses a grate furnace (SHA, SEGHERS, Willebroek, Belgium) and

the resulting solid residues consist of about 30 tons of fly ash and 150–250 tons of bottom ash per day. The furnace is equipped with an air pollution control system that includes a semi-dry flue gas cleaning tower, an active carbon adsorption reactor, and a bag filter. The fly ash is a mixture of ash from the gas cleaning tower and the bag filter.

The chemical characterization of the original fly ash was conducted using X-ray fluorescence (XRF-1700, Shimadzu Corporation, Kyoto, Japan) for the major elements (Na, K, Ca, magnesium (Mg), silicon (Si), ferrum (Fe), Al, Cl) and SO_3, and the analyses were carried out in triplicate. The minor elements were determined using inductively coupled plasma-mass spectrometry (ICP-MS, SERIES, Thermo Scientific, Waltham, United States) after microwave digestion. The microwave digestion was conducted on duplicate samples and compared with a blank sample without MSWI fly ash addition. The ICP-MS results were determined as the average of the measurements and were shown in Table 1. Results smaller than 1% are not listed.

The main elements of the fly ash were similar to that of natural minerals.[12] Among the trace elements, Zn, Pb and Cu were the most abundant; these are easily dissolvable. Other trace elements (Cd, antimony (Sb) and molybdenum (Mo)) were less abundant, but are also dissolvable.

The fly ash had a high chloride and sulfate content of 18.88% and 5.18%, respectively. The chloride in the fly ash primarily came from the municipal solid waste, including sodium chloride (NaCl) in kitchen waste and plastic, rubber and leather.[17] During combustion, the organic chloride was converted into hydrogen chloride (HCl) and small amounts of chloride (Cl_2), while a portion of the inorganic chloride was converted into HCl, and the remainder condensed on the surface of the fly ash and slag.[19]

Table 1 Chemical composition (major and minor elements) of MSWI fly ash

2.2 Washing experiment

To assess the effectiveness of the washing process for removing chloride and sulfate from the fly ash, ash and deionized water were mixed to obtain specific L/S ratios (L/kg), after which each mixture was put into a polyethylene bottle. The bottle was then sealed and placed on a level platform shaker to induce horizontal oscillation at a constant frequency of 110±10 times·min^{-1} and amplitude of 20 mm. The experiments were conducted at room temperature. The orthogonal test were used to indentify the optimium washing conditions, the orthogonal experimental design and

the results were shown in Table 5, The $L_{16}(4^2)$ orthogonal array were constructed, thus 2 factors and 4 levels were used to do the orthogonal experiment. The washing durations were 5 min,10 min, 30 min, 1 h and the L/S ratios were 3, 5, 10, and 20. The influence of the washing temperature were also investigated in this paper, the experiments were onducted at 25^{o}C, 35 ^{o}C,45 ^{o}C,55 ^{o}C,70 ^{o}C,85^{o}C , respectively at the optimium washing conditions. The resulting wastewater from each L/S-duration combination was analyzed individually. First, a small quantity of wastewater was removed and acidified with 10% nitric acid to a pH of less than 2 for analysis of trace elements with ICP-MS. The remaining bulk wastewater from each mixture was filtered through 0.45 μm membrane filters for chloride and sulfate analyses. The chloride and sulfate were analyzed using ionic chromatography (Dionex - 100, Dionex, Sunnyvale, United States). All analyses were conducted in triplicate.

The Na^+, K^+, and Ca^{2+} in the wastewater were determined by inductively coupled plasma-atomic emission spectrometry (ICP-AES, PRODIGY Type, Thermo Electron, Waltham, United States). The critical trace elements (Zn, Pb and Cu) in the wastewater from the washing process were evaluated by ICP-MS (Thermo Scientific).

2.3 Precipitation of trace elements in the wastewater

The trace elements Cu, Zn and Pb were precipitated using two methods:

1) Bubbling CO_2 into the wastewater: Analytical grade CO_2 gas was bubbled from a submerged gas membrane through wastewater samples at each of three flow rates (40, 10 and 5 mL·min^{-1}) controlled by a mass flow controller (D07-7B, Sevenstar Electronics, Beijing, China). Samples were continuously stirred at a constant rate of 200 rpm using a Teflon-coated magnetic stirring bar. The pH of the solutions was measured using a pH meter and was observed to decrease continuously as the carbonate precipitation process progressed.
2) Sodium carbonate solution: Two concentrations (1 mol·L^{-1}, 0.1 mol·L^{-1}) of sodium carbonate solution were added to wastewater samples using a peristaltic pump to deliver sodium carbonate solution at three different rates (0.001 mol·min^{-1}, 0.0025 mol·min^{-1}, 0.0001 mol·min^{-1}).

Precipitated solids were separated from the wastewater by filtering the wastewater through membrane filters (0.45 μm). The residue was dried at 105°C for 24 h, after which it was analyzed.

Following the separation of precipitated solids, the resulting leachate was acidified with 10% nitric acid to a pH of less than 2 for the analysis of trace elements.

Scanning electron microscope (SEM) observations were made on carbon-coated co-precipitation products using secondary electron imaging. The resolution was 6 nm, and the voltage was 20 KV (S-450, Hitachi, Tokyo, Japan).

X-ray diffraction (XRD) examinations on samples were conducted using a D/max-2500 diffractometer using Cu Kα radiation (U = 50 keV, I = 200 mA) to identify the crystal phases of the precipitates. Scans were conducted from 10° to 70° at a rate of 4° $2\theta \cdot min^{-1}$ (Rigaku, Osaka, Japan).

The mineralogical inventory and the distribution of trace elements in the precipitates were identified using a Scanning Electron Microscope equipped with an Energy-Dispersion Spectrometer (SEM-EDS) with voltage of 15 kV and a resolution of 1.5 nm (JSM 6301, JEOL, Tokyo, Japan). The samples were polished carefully in an automatic metallographic grinding and polishing machine until the majority of the samples had a hemispheric shape, as observed under a microscope. Before examination, the samples were covered with carbon to facilitate the observation of carbonates.

2.4 Modeling the co-precipitation of trace elements

The precipitation behavior of trace elements was modeled using PHREEQC (2.15),[20] a geochemical code. This diffuse double-layer model (DLM) elucidates the boundary layer that exists between solids in a solution and the aqueous phase, independently of the surface charge of the solids. In reality, high concentrations of cations and anions exit within the diffuse layer due to electrostatic forces.

Solid-solutions are significant for scavenging trace elements from water and for limiting the kinesis of trace elements in the environment. For the calculation of solid-solution mineral behavior, the site-mixing model (in which substituting elements can replace certain elements only at certain sites within the crystal structure) can be used to describe the removal of trace elements by calcite.

In the present study, co-precipitation with calcite is modeled in combination with the 'solid solution' selection from the PHREEQC model. All solid solutions formation were considered for (Ca, Cu)CO_3, (Ca, Pb)CO_3, (Ca, Zn)CO_3, Palacha et al.[21] estimated Pb and Zn mixing parameters, which Guggenheim parameters was calculated to be a_0= 2.94 and 3.56, for Cu we use Zn parameters as a reference due to lack of thermodynamic data. The PHREEQC model was also used to evaluate

the surface complexation of trace element onto Fe/Al colloids from the process of carbonation of wastewater generated from washing MSWI fly ash. The calculations were based on the DLM, together with Dzombak and Morel's [22] database of sorption constants for HFO, which is incorporated into the PHREEQC computer code. The sorption database for hydrous ferric oxide (HFO) has been used previously for modeling the leaching of trace elements from incineration residues.[23-25]

The input contents of constituents were based on the maximum leaching capacity in the MSWI fly ash and are given in Table 2. The temperature is set as 298.15 K. Thermodynamic data of solution species used to define association reaction for aqueous species are shown in Table 3 and phase used to define mineral shown in Table 4. Selection The Hfo was defined by Goethite and the concentration of HFO is the amount of Goethite ($Fe(OH)_3$), the Surfa was defined by Gibbsite and the concentration of Surfa is the amount of Gibbsite ($Al(OH)_3$). Two types of binding sites were defined for a surface: strong binding sites and weak binding sites. To maintain consistency with their model, the relative number of strong and weak sites was kept constant as the total number of sites varied. HFO was not measured in the experiment but was theoretical calculate in PHREEQC based on the input file. Other parameters including surface species, phase, solution species and solid solution species are listed as supporting materials.

Table 2 The input data of the modeling (water=1kg)

Table 3 Solution species used to define association reaction for aqueous species

Table 4 Phase used to define mineral

3. Results and discussion

3.1 Release of total dissolved solids (TDS) and critical trace elements during the washing of fly ash

The release of TDS at different L/S ratios and different washing durations is illustrated in Fig. 1. The TDS in the original fly ash and washed fly ash, as determined by XRD analysis, were comprised mainly of halite (NaCl), sylvite (KCl), anhydrite ($CaSO_4$) and calcium chloride hydroxide (CaClOH). The wastewater produced by the washing process had high concentrations of Ca^{2+} due to the presence of TDS. Specifically, as the L/S ratio increased from 3 to 50, TDS increased from about

20% to 37%. The washing duration had no significant effect on the TDS content of wastewater at a given L/S ratio. For example, as the washing duration increased from 10 min to 16 h, TDS only slightly increased from 19.6% to 22% at L/S = 3 and from 34.7% to 36.9% at L/S = 50. Salts of Na, K and Ca showed similar behaviors when the fly ash was washed, and all of these elements nearly reached their maximum concentrations after washing for only a very short duration. As a result, as the washing duration increased, TDS increased only marginally. These results are compatible with the previous research by Kirby and Rimistidt[15] on the reaction of incineration fly ash with water. They found that the release of Na, K and Cl was primarily controlled by the availability of soluble salt, while Ca release was controlled by the availability of soluble salt or solubility under a lower L/S ratio.

In the present experiment, when the fly ash interacted with water for only a very short time the pH of the suspension reached 11.8 because of the portlandite in the fly ash (Fig. 1). The washing duration had little effect on the pH of the suspension, as indicated by a change of only 0.3 over the range of washing durations. As the L/S ratio increased, the pH of the suspension increased, with a dramatic increase being observed before an L/S ratio of 10. Conversely, the pH remained steady with L/S ratios greater than 10. The dissolution of portlandite explains the high initial pH values, which were close to pH 12.3.

Fig. 1. TDS content (wt %) and pH of the wastewater from MSWI fly ash washing as a function of L/S ratio and washing duration. The solid symbols represent pH; the hollow symbols represent TDS.

The chloride and sulfate extraction results are shown in Table 5, which presents the amount leached in the water as a function of the L/S ratio and washing duration. The chloride and sulfate anions tended to be deposited on the surface of the fly ash particles and were easily removed during washing. Thus, the increase in the L/S ratio produced the expected increase in chloride and sulfate extraction independently of washing duration. The extraction of chloride at L/S ratios of 3 and 20 was 58.5% and 85.4%, respectively. The extraction of sulfate was less than 50% that of chloride, even at an L/S ratio of 20.

In the Table 6, K_j represents the experimental indicator when each parameter is at levels 1–4, R is the difference between the lowest value and the highest value for each parameter. By comparing the R-values of each fact, it can be found that the L/S ratio was the significant parameter, which

influence the extraction of Cl^- and SO_4^{2-}. For the remove of Cl^-, it is clear that K-value reached a maximum value at the third level, hence the optimum L/S ratio for Cl^- remove is 10, although K-value reached a maximum value when washing duration was 1h, but considering time consumption, the optimum washing duration could be 10 min. However for the remove of SO_4^{2-}, The optimum washing condition was an L/S ratio of 20 for 10 min. The main purpose of the fly ash water washing was to remove chlorine, thus he optimum washing condition was an L/S ratio of 10 for 10 min.

Table 5 Orthogonal experimental design and the results

Table 6 Parameters of orthogonal experiment

Fig. 2 shows the chloride and sulfate extraction results as a function of temperature. The washing durations were 10 min at L/S = 10, and experiments were onducted at 25°C, 35 °C, 45 °C, 55 °C,70 °C,85°C , respectively. the increase in temperture produced the expected increase in chloride extraction. The extraction of chloride at temperture of 25°C and 85°C was 83.4% and 94.5%, respectively. However sulfate extraction showed a opposite characteristics as temperture increased. The extraction of sulfate at temperture of 25°C and 85°C was 29.7% and 24.1%, respectively.

Fig. 2. Extraction of chloride and sulfate from MSWI fly ash as founction of temperture

Considering orthogonal experimental results, wastewater from an L/S ratio of 10 was selected for investigating the extraction of trace elements (Pb, Zn and Cu). At L/S = 10, washing duration had no significant effect on the trace element concentration in the resulting wastewater. The Pb concentrations across the spectrum of washing durations ranged from 43.4 to 63.7 $mg \cdot L^{-1}$, the Zn concentrations ranged from 3.4 to 4.8 $mg \cdot L^{-1}$, and the Cu concentrations ranged from 0.40 to 0.53 $mg \cdot L^{-1}$. As shown in Fig. 1, the washing duration had little effect on the dissolution of soluble salts. Because it is economical to minimize the washing duration, 10 min was selected as the optimum washing duration. At this washing duration and an L/S of 10, the concentrations of Pb, Zn and Cu ions were 63.7 $mg \cdot L^{-1}$, 4.53 $mg \cdot L^{-1}$ and 0.40 $mg \cdot L^{-1}$, respectively. The concentrations of Pb , Zn and Cu were higher than those allowed (0.1 $mg \cdot L^{-1}$, 0.1 $mg \cdot L^{-1}$ and 0.01 $mg \cdot L^{-1}$, respectively) in the

discharge standard for a municipal wastewater treatment plant.

3.2 Co-precipitation of trace elements by adding Na_2CO_3

To remediate contaminated MSWI fly ash waste water, toxic trace elements might be removed from the waste water by co-precipitation with calcite in a mixed flow reactor, where a sodium carbonate solution is mixed with wastewater, causing $CaCO_3$ precipitation. This process does not change the pH of the wastewater, as shown in Eqn. 1:

$$Ca(OH)_2 + Na_2CO_3 = CaCO_3 \downarrow + 2NaOH \quad (1)$$

Using an sodium carbonate solution to precipitate trace elements results in only two possible precipitation ways, namely formation of a carbonate of the trace element and adsorption onto (or incorporation into) the resulting calcite carbonate. No colloids of Fe or Al are generated, nor are trace-element hydroxides. Hence the adsorption of trace elements on colloids of Fe or Al and trace-element hydroxides does not occur during the process.

The results from adding sodium carbonate to the fly ash wastewater are shown in Fig. 3. Trace elements Cu, Zn and Pb are strongly incorporated into calcite carbonate. Eqn. 2 shows that the tendency for calcite to sequester a trace element is based on the ratio of the solubility product of calcite to the solubility product of the trace element mineral, and is related to the amount of Ca precipitated from the solution. In the present study, the initial concentration of Na_2CO_3 was 1 $mol \cdot L^{-1}$. Even though only a very small amount of Na_2CO_3 was added, the $CaCO_3$ precipitated rapidly, and the trace element content was reduced to a very low concentration. To highlight the trace element behavior more clearly, the concentration of Na_2CO_3 solution was reduced to 0.1 $mol \cdot L^{-1}$ and the flow rate at which it was added to the waste wash water was reduced to 1 $mL \cdot min^{-1}$. The results clearly demonstrated that even when a very small amount of Ca^{2+} in the wastewater precipitated, the trace element concentrations decreased significantly. Because Cu, Zn and Pb can form insoluble carbonate products, they are the elements most strongly sequestered.

Calcite is an important substance for sequestering trace elements, either via physical adsorption related to pH, false isomorphism (independent of input or time) or co-precipitation.[26] The incorporation of trace elements into the calcite lattice can retard their migration much more effectively than can simple adsorption.[27]

In the geological science field, many studies have examined the sequestration or adsorption of

trace elements in calcite in natural water systems, both saline and non-saline.[15] The pH of sea water is usually in the range of 7.9–8.4, while that of freshwater systems is usually in the range of 6–8. In the present study, the pH of the waste wash water was high (approximately 12), which is much different from that of natural water systems. Though the model introduced by Rimstidt et al.[28] to describe the co-precipitation of trace elements as a function of the distribution coefficient (K_d) and fraction of metallic carbonate (MCO_3) is based on natural water systems it still has the efficacy in an experimental condition with an important point that the pH of the water system is relatively unchanged by the reaction.

Fig. 3. Fraction of trace elements remaining in the waste wash water (f_{Tr}) after the addition of Na_2CO_3 as a function of the fraction of Ca removed (F_{Ca}). Fig. 3(a) Cu removal; Fig. 3(b) Pb removal; and Fig. 3(c) Zn removal. Initial Cu concentration ($C_{0,Cu}$) = 0.40 mg·L^{-1}; initial Pb concentration ($C_{0,Pb}$) = 63.7 mg·L^{-1}; initial Zn concentration ($C_{0,Zn}$) = 4.53 mg·L^{-1}.

The results obtained for Cu indicated that K_d is 31 for a 1 mol·L^{-1} sodium carbonate solution added at the rate of 2.5 mL·min^{-1}, and K_d is 120 for a 1 mol·L^{-1} sodium carbonate solution added at the rate of 1 mL·min^{-1}. According to the measured value of K_d, the amount of trace element retained in the wastewater (f_{Tr}) was plotted as a function of the fraction of Ca removed (F_{Ca}) from the wastewater (Fig. 3(a)). The fourfold difference in K_d values demonstrates that the precipitation rate has a significant effect on K_d. The decrease in K_d with increasing precipitation rate is consistent with a solution boundary-layer-related process. Similarly, the K_d for Zn is 21 for a 1 mol·L^{-1} sodium carbonate solution added at the rate of 2.5 mL·min^{-1}, and 65 for a 1 mol·L^{-1} sodium carbonate solution added at the rate of 1 mL·min^{-1}. The K_d for Pb is 7.5 for a 1 mol·L^{-1} sodium carbonate solution added at the rate of 2.5 mL·min^{-1}, and 5 for a 1 mol·L^{-1} sodium carbonate solution added at the rate of 1 mL·min^{-1}. Because the trace elements Cu, Zn and Pb each have an ionic radius smaller than Ca^{2+} they fit into the calcite lattice more easily. The effective ionic radii for Ca^{2+}, Cu^{2+}, Zn^{2+}, Pb^{2+} are 1.00, 0.73, 0.74, and 1.18 respectively.[29] Thus, these trace elements are incorporated into calcite in the following order: $Cu^{2+} > Zn^{2+} > Pb^{2+}$, which is consistent with the order of their effective ionic radii.

3.3 Co-precipitation of trace elements with $CaCO_3$ and Fe/Al colloids by bubbling CO_2

Fig. 4(a) illustrates the precipitation of Ca using CO_2. For the experiments, CO_2 was bubbled at a rate of 10 mL·min^{-1} into 50 mL of waste wash water. As washing duration increased, the Ca^{2+} ions in the resulting wash water precipitated more quickly because the reaction between the CO_2 and Ca^{2+} ions generated calcite. The reactions involved in the carbonation process are listed below:

$$Ca(OH)_2(s) \rightarrow Ca^{2+} + 2OH^- \quad (2)$$

$$CO_2(g) \rightarrow CO_2(l) \quad (3)$$

$$CO_2(l) + OH^- \rightarrow HCO_3^-(l) \quad (4)$$

$$HCO_3^-(l) + OH^- \rightarrow H_2O(l) + CO_3^{2-} \quad (5)$$

$$Ca^{2+} + CO_3^{2-} \rightarrow CaCO_3(s) \quad (6)$$

The controlling step in the carbonation process is the dissolution of the CO_2 (as described in Eq. (3)).[30] Dissolution of the CO_2 leads to consumption of OH^- ions according to Eq. (4) and Eq. (5), which leads to generation of $CaCO_3$ with spherical shapes of diameter 10 μm. In the present study, when there was no reaction between precipitated $CaCO_3$ and CO_2 to form calcium bicarbonate ($Ca(HCO_3)_2$), the removal ratio of Ca (F_{Ca}) reached its maximum value.

Fig. 4(b) shows the change in the conductivity and pH of waste wash water in response to CO_2 bubbling as a function of time. The conductivity and pH decreased very slowly when CO_2 was introduced into the solution and stirred with a magnetic stirrer. The reaction of $Ca(OH)_2$(aq) with CO_2 was a velocity-controlled process that primarily occurred near the gas membrane. Calcite precipitation decreased the amount of Ca ions in solution, with a resultant decrease in pH. When the reaction of $Ca(OH)_2$(aq) with CO_2 was complete, the conductivity and pH of the solution decreased sharply. When generation of the $Ca(HCO_3)_2$ began, the conductivity increased again, while the pH decreased very slowly again until the generation and dissolution of $CaCO_3$ reached equilibrium.

Fig. 4. Conductivity and pH in waste wash water (L/S ratio=10, washing duration=10 min) as a function of time while bubbling CO_2 into the wastewater at a flow rate of 10 mL·min^{-1}. Fig. 4(a) shows the removal ratio of Ca (F_{Ca}); Fig. 4(b) shows the pH and conductivity change. The square points represent pH, and the circular points represent conductivity.

Fig. 5(a)–(c) illustrate the co-precipitation of Cu, Pb and Zn in terms of the fraction of trace element retained (f_{Tr}) as a function of the fraction of Ca removed (F_{Ca}) when CO_2 was bubbled into the waste wash solution at different flow rates. As shown, only a small amount of Ca^{2+} was precipitated at the CO_2 flow rate of 40 $mL \cdot min^{-1}$, while the retention ratio of the Zn was reduced to 0.2.

Fig. 5. Trace elements retained in the waste wash water when CO_2 was bubbled at different flow rates. In these figures, the horizontal axis is the Ca^{2+} removal ratio (F_{Ca}), while the vertical axis is the dimensionless settled fraction of trace element in the waste water (f_{Tr}, where f is the retained fraction and Tr is the trace element).

Fig. 6(a)–(c) illustrates the co-precipitation of Cu, Pb and Zn in terms of the solution concentration of these elements as a function of pH when CO_2 was bubbled into the waste wash water at different flow rates. As shown, only a small decrease in pH led to enormous decreases in the trace element concentrations. There were insufficient concentration data in the pH range of about 7.5-11 because the concentrations of all three elements decreased sharply when pH decreased from 12 to 11, which can be seen clearly in Fig. 4(b).

Fig. 6. Trace elements (Cu, Pb and Zn, respectively) concentration as pH changed.

Fig. 7(a) illustrates the adsorption of Cu ions on Fe/Al colloids, and the co-precipitation of Cu ions with $CaCO_3$ in terms of the fraction of Cu composition as a function of pH. Initially, the bubbling of CO_2 caused precipitation of Cu ions ($Cu(OH)_2$) from the solution. In the pH range of 10–12 adsorption of Cu was indistinct on colloids of Fe/Al. The removal ratio of Cu by $Fe(OH)_3$ and $Al(OH)_3$ increased quickly at pH <10 due to the rapid formation of $Al(OH)_3$(s). The co-precipitation of Cu with $CaCO_3$ was smaller than the adsorption of Cu by $Al(OH)_3$ and $Fe(OH)_3$ in pH range 6.7-10,but was the mainly solubility- control mechanism at pH values blow 6.7.

Fig. 7(b) shows the possible solubility-control mechanism in terms of the fraction of Pb removed as a function of pH. The processes that decreased the Pb ion concentration in aqueous solution were precipitation of $Pb_2(OH)_3Cl$ hydroxide based on the pH change, and adsorption of Pb on Fe/Al colloids, and co-precipitation of Pb with $CaCO_3$. $Pb_2(OH)_3Cl$ will form when the pH of the solution decreases and the solution is oversaturated with Pb ions. $Fe(OH)_3$ and $Al(OH)_3$ will generate at pH<10.6, have the same adsorption capacity for trace elements, Surface reaction Equations (Table 7)

show the adsorption balance of HFO on Pb^{2+}. In the present study, the adsorption effect was only obvious at pH between 6.5 and 10.6. The adsorbed Pb^{2+} increased with an increasing molar concentration of Fe/Al colloids, which agrees with previously reported results. [31]An obvious adsorption effect can be observed when the molar concentration of a colloid is five times higher than that of the trace element.[32, 33]Because in the present study, the molar ratio of colloids to Pb^{2+} was only 0.58, the adsorption of Pb^{2+} by the colloids was limited.

$CaCO_3$ can adsorb trace elements by incorporating the trace element ions into the calcium carbonate crystal and replacing the original Ca ions, thus resulting in calcium carbonate crystal precipitation.[34] In the present study, The amounts of $Fe(OH)_3$ and $Al(OH)_3$ generated in the waste wash water were far less than the amount of $CaCO_3$ produced because the Ca^{2+} concentration in solution was three and four magnitudes higher than the concentrations of Al^{3+} and Fe^{3+}, respectively. The major cause of Pb^{2+} precipitation in solution was this element's co-precipitation with $CaCO_3$ at lower pH.

Fig. 7(c) illustrates Zn concentration is mainly influenced by solubility control from $Zn(OH)_2$ between 11.4 and 12.2 and Zn_2SiO_4 around pH 11.4 -7.3. Generally willemite (Zn_2SiO_4) is close to saturation above pH 7 and has been suggested for solubility control,[35] however at high pH(11.4-12.2) Zn concentration can be predicted by $Zn(OH)_2$, Van Herck et al.[36] found that in high pH the formation of hydroxide complexes was responsible for the solubility- control. While the adsorption of Zn ions onto $Fe(OH)_3$ and $Al(OH)_3$ began to increase quickly and get a maximum value at pH of 7.4. The formation of $Ca_{(X)}Zn_{(1-X)}CO_3(s)$ began to increase when the pH decreased below 8 and became the major precipitation phase when the pH decreased below 7.

Fig. 7. The modeling results predicting the behavior of Cu, Pb and Zn, respectively. The solid line represents the solution of a trace element, and the dotted lines are the single case of a trace element. (Abbreviations used in the figure are: "pre" = precipitation and "Ads" = adsorption.)

Table 7 Surface species used for association reaction in solution mode

Table 8 shows the corresponding minimum trace element concentrations when CO_2 was bubbled at the flow rate of 40 $mL \cdot min^{-1}$, 10 $mL \cdot min^{-1}$, and 5 $mL \cdot min^{-1}$. At the high CO_2 bubbling flow rate (40 $mL \cdot min^{-1}$), the concentrations of Cu and Zn were significantly lower than the allowable discharge limits for these elements in treated municipal wastewater. The minimum

concentration of Pb was the same as the discharge limit (but the initial concentration of this element was much higher than the discharge limit).

Table 8 Minimum concentrations ($mg \cdot L^{-1}$) of trace elements in waste wash water after CO_2 bubbling.

3.4. Comparison of the two methods

It is interesting to note that for Zn, the retention ratio initially decreased, then increased, and decreased again as the amount of Ca removed from solution progressively increased. The effect of bubbling CO_2 on Zn precipitation in the waste wash water is clearly illustrated in Fig.5(c).

The removal of Pb by CO_2 bubbling was effective to a certain extent. When the removal ratio of Ca^{2+} was 0.72, the retention ratio of Pb in the solution decreased to 0.07. Similarly, the retention ratio of Cu in the wash water solution was 0.5 when only 2.98% of Ca^{2+} was removed, but the Cu retention ratio decreased dramatically to 0.17 when just 12.8% of Ca^{2+} was precipitated.

In comparison, bubbling of CO_2 through waste fly ash wash water had the advantage over adding sodium carbonate by reducing both the concentrations of critical trace elements and the solution pH simultaneously.

3.5. Morphology and mineralogy of the precipitates

Fig. 8 shows the morphologies of $CaCO_3$ particles precipitated from wastewater of the washing process with a 10 min washing duration at different L/S ratios. The L/S ratio of the washing process affected the shapes of the $CaCO_3$ precipitation products. When the L/S ratio was 3, the shape of precipitated $CaCO_3$ was a spindle; when the L/S ratio was 10, the shape of $CaCO_3$ was spherical with a diameter between 4 μm and 10 μm; when the L/S ratio was 20 the shape of $CaCO_3$ was tubular.

Fig. 8. Morphology of $CaCO_3$ precipitated from ash washing wastewater. The CO_2 flow rate was 40 $mL \cdot min^{-1}$.The washing duration was 10 min. Fig. 8(a) L/S = 3; Fig. 8(b) L/S = 10; Fig. 8(c) L/S = 20.

Fig. 9 shows the XRD diffractogram of the precipitated sediments resulting from treating the waste wash water by adding Na_2CO_3 solution to the wastewater and by bubbling CO_2 into the

wastewater. The diffractogram showed that the main component of these sediments was $CaCO_3$, regardless of the treatment method. In the diffractogram of sediment generated by adding the Na_2CO_3 solution, NaCl was identified. This may have been because during the precipitation of $CaCO_3$ the sediments absorbed small amounts of water that was abundant in NaCl. This sediment also contained lead oxide (PbO). The first strong peak of PbO was at about 28°, which overlapped with the main peak of $CaCO_3$. Moreover, there was no single strong peak of Pb that did not overlap other phases. Neither Zn nor Cu was apparent in the diffractogram for this sediment, meaning that the content of Zn and Cu in the sediment was lower than the detecting limit of XRD (about 3%). The XRD analysis and SEM observations revealed that $CaCO_3$ was the only precipitate formed during the precipitation experiment.

Fig. 9. XRD diffractogram of precipitation sediments from the treatment of fly ash wash water. Fig. 9(a) is the diffractogram of sediment precipitated by adding Na_2CO_3 solution to the wastewater. The washing duration was 10 min and L/S = 10. Fig. 9(b) is the diffractogram of sediment precipitated by bubbling CO_2 at a flow rate of 40 $mL \cdot min^{-1}$ into the wastewater. The washing duration was 10 min and L/S = 10. Fig. 9(c) is the diffractogram of sediments precipitated by bubbling the CO_2 at a flow rate of 40 $mL \cdot min^{-1}$ into the wastewater. The washing duration was 10 min and L/S = 3.

3.6. SEM-EDS analysis of the precipitate

Based on the XRD patterns, conclusions could not be made about which mechanism controlled the precipitation of Pb, Zn and Cu; thus, SEM-EDS analysis was performed to identify this mechanism. Fig. 8 revealed that the sediments were mainly spherical with a diameter between 4 μm and 10 μm. As shown in Fig. 9, the co-precipitation products generated by bubbling CO_2 were all calcite, but with different crystal phases. The EDS analysis failed to detect Mg in any precipitate generated in the wastewater treated by CO_2 bubbling, but did identify small amounts of Si and Cl in some sediment.

To investigate the distribution of trace elements in the spherical $CaCO_3$ precipitation products, these were ground into hemispheres and analyzed. In the precipitation of calcium carbonate three anhydrous crystalline polymorphs are known to form. They are, in order of increasing stability, vaterite, aragonite, and calcite. Spontaneous precipitation by the mixing of two concentrated solutions of calcium or bubbling CO_2 into Ca ion rich solutions and carbonate results in a gelatinous

matter when ionic activity product (IAP) exceeds the solubility product (KSP) of amorphous calcium carbonate. Spherical and cubic $CaCO_3$ generation was mainly due to the interaction of differentions in the electrolyte, if the reaction system was filtered immediately without aging then ions are attracted to each other in all directions, forming a spherical $CaCO_3$ particles. If after a period of time aging, $CaCO_3$ crystal formation harness bar, then formed cubic $CaCO_3$, because cubic $CaCO_3$ is the most stable natural $CaCO_3$ (calcite) with the minimum molecular surface energy.[37-40] Fig. 10 shows the back-scattered image of one typical hemisphere, and Table 9 shows the analytical results. The EDS spectra revealed the presence of Ca, Al, C, O, S, Cl, Pb and antimony (Sb).

Additionally, the concentration of Pb increased from the outer layer of the precipitate to its center, as did the concentration of Ca. The concentration of C showed the opposite trend, with the highest concentration of C found on the outer layer of the precipitates.

To identify the Pb related phase, XRD diffraction was conducted again using a slow scanning speed of 2° 2θ·min^{-1}. However, no Pb-related phase was identified. More important, no Fe was detected by SEM-EDS analysis of the precipitate resulting from bubbling CO_2 into the wastewater. However, the precipitate contained Al ranging from 0.52% to 2.01% which may confirm the adsorption of trace element ions onto $Fe(OH)_3$ and $Al(OH)_3$.

It was very interesting that the precipitates were enriched with antimony (Sb). Leachable Sb is strongly dependent on pH; a maximum concentration has been observed at near-neutral pH (approximately 8–10) but lower concentrations at extremely high and extremely low pH.[23, 41] At high pH and in oxidizing conditions, Sb is likely to form oxyanions, such as $Sb(OH_6)^-$.[42] The CO_2 bubbling into the wastewater led to the precipitation of Fe/Al-hydroxides. Fe/Al-hydroxides may bind Sb ions by sorption as well as by co-precipitation processes.[43]

Fig. 10. SEM-EDS analysis of a typical sphere of the precipitate formed during treatment of waste fly ash wash water by CO_2 bubbling. Fig. 10(a) is a back-scattered image of the precipitate; Fig. 10(b) is the EDS analysis of the precipitate.

Table 9 Chemical composition of the precipitate formed during treatment of waste fly ash wash water by CO_2 bubbling.

4. Conclusions

This study examined washing followed by CO_2 bubbling as techniques to remove three amphoteric trace metals (Pb, Zn and Cu) from MSWI fly ash. These elements typically occur in the highest concentrations in MSWI fly ash, easily leach in highly alkaline conditions, and readily combine with chloride ions in aqueous solutions.

The total dissolved solids accounted for 20%–37% of the original MSWI fly ash (w/w) during the washing process as the L/S ratio increased from 3 to 50. The pH of the wastewater from the washing process increased as the L/S ratio increased, and reached 12.5 when the L/S ratio was 50. The TDS were comprised of Ca-, Na- and K-related compounds and were released quickly over a very short time.

The wastewaters generated from washing fly ash in this study had a high concentration of $Ca(OH)_2(aq)$; therefore, they easily generated calcite when CO_2 was bubbled into them. Calcite precipitation effectively reduced the pH of the wastewater.

The accelerated precipitation of calcite or Al-hydroxides was responsible for the removal through co-precipitation of amphoteric trace elements (Pb, Cu and Zn) from wastewaters generated from washing MSWI fly ash. The precipitated calcite consisted primarily of spheres with a diameter between 4 μm and 10 μm and formed in different shapes including spheres, spindles and tubes depending on the L/S ratio of the washing process. The SEM-EDS analysis of the precipitate revealed that the Pb concentration increased from the outer to the inner part of the sphere along a radial direction. The XRD analysis did not reveal any Pb-related crystal phase in the precipitate.

A chemical and mineralogical analysis (SEM/EDS, XRD, and ICP-AES) revealed that co-precipitation is an important method for spontaneous decontamination of wastewater generated from the fly ash washing process. The removal of contaminants occurs especially when the wastewater exhibits both high alkalinity and high trace element concentrations.

The manuscript focuses on the fate of three amphoteric trace metals (Pb, Zn and Cu) in the wastewater, which get the highest concentrations in MSWI fly ash larger than 1000 $mg \cdot kg^{-1}$. They can be removed using the tail gas of cement kilns, which are primarily composed of CO_2. While it must be pointed out that MSWI fly ash leachate contains also other contaminants that are presently

not treated in the manuscript. For instance, antinomy gets the fourth concentration just lower than 1000 $mg \cdot kg^{-1}$, Cadium get a value of 97 $mg \cdot kg^{-1}$, they two can potentially be a problem as compared to existing leaching limit values. Also other contaminants such as cadium, barium, molybdenum, arsenic, vanadium, selenium can be present in environmentally relevant concentrations, though they get a lower concentration in MSWI fly ash. The co-precipitation behavior of other trace elements during the neutralization of highly alkaline MSWI fly ash wash water using CO_2, or industrial waste gases that are rich in CO_2, needs further comprehensive investigation.

Acknowledgments:

Financial support from the National Science Foundation (No. 51108276) and the National Basic Research Program of China (No. 2011CB201500) in China is acknowledged.

References:

1. O. Hjelmar, *Journal of Hazardous Materials*, 1996, **47**, 345-368.
2. Y. S. Liu, L. T. Zheng, X. D. Li and S. D. Xie, *Journal of Hazardous Materials*, 2009, **162**, 161-173.
3. P. Freyssinet, P. Piantone, M. Azaroual, Y. Itard, B. Clozel-Leloup, D. Guyonnet and J. C. Baubron, *Waste Management*, 2002, **22**, 159-172.
4. R. Kikuchi, *Resources Conservation and Recycling*, 2001, **31**, 137-147.
5. C. A. Sikalidis, A. A. Zabaniotou and S. P. Famellos, *Resources Conservation and Recycling*, 2002, **36**, 155-167.
6. N. Saikia, S. Kato and T. Kojima, *Waste Management*, 2007, **27**, 1178-1189.
7. X. B. Gao, W. Wang, T. M. Ye, F. Wang and Y. X. Lan, *Journal of Environmental Management*, 2008, **88**, 293-299.
8. J. R. Pan, C. P. Huang, J. J. Kuo and S. H. Lin, *Waste Management*, 2008, **28**, 1113-1118.
9. L. Wang, Y. Y. Jin and Y. F. Nie, *Journal of Hazardous Materials*, 2010, **174**, 334-343.
10. E. Mulder, *Waste Management*, 1996, **16**, 181-184.
11. T. Mangialardi, *Journal of Hazardous Materials*, 2003, **98**, 225-240.
12. J. A. Meima, R. D. van der Weijden, T. T. Eighmy and R. N. J. Comans, *Applied Geochemistry*, 2002, **17**, 1503-1513.
13. Z. Abbas, A. P. Moghaddam and B.-M. Steenari, *Waste Management*, 2003, **23**, 291-305.
14. J. M. Chimenos, A. I. Fernández, A. Cervantes, L. Miralles, M. A. Fernández and F. Espiell, *Waste Management*, 2005, **25**, 686-693.
15. C. S. Kirby and J. D. Rimstidt, *Environmental Science & Technology*, 1994, **28**, 443-451.
16. K. S. Wang, K. Y. Chiang, K. L. Lin and C. J. Sun, *Hydrometallurgy*, 2001, **62**, 73-81.
17. Z. Yang, Master, Zhejiang University, 2003.
18. M. Todorovic and H. Ecke, *Waste Management*, 2006, **26**, 430-441.
19. S. Uchida, H. Kamo and H. Kubota, *Industrial & Engineering Chemistry Research*, 1988, **27**, 2188-2190.
20. D. L. Parkhurst and C. A. J. Appelo, PHREEQC(version2.15) Denver CO, U.S., 2009.

21. C. Palache , H. Berman and C. Frondel *The System of Mineralogy*, Wiley & Sons, New York, 1951.
22. D. A. Dzombak and F. M. M. Morel, *Surface Complexation Modeling: Hydrous Ferric Oxide*, John Wiley and Sons, New York, 1990.
23. J. A. Meima and R. N. J. Comans, *Journal of Geochemical Exploration*, 1998, **62**, 299-304.
24. B. Van der Bruggen, G. Vogels, P. Van Herck and C. Vandecasteele, *Journal of Hazardous Materials*, 1998, **57**, 127-144.
25. J. J. Dijkstra, H. A. van der Sloot and R. N. J. Comans, *Waste Management*, 2002, **22**, 531-541.
26. U. Forstner and S. R. Patchineelam, *Chemiker-Zeitung*, 1976, **100**, 49-57.
27. A. J. Tesoriero and J. F. Pankow, *Geochimica Et Cosmochimica Acta*, 1996, **60**, 1053-1063.
28. J. D. Rimstidt, A. Balog and J. Webb, *Geochimica Et Cosmochimica Acta*, 1998, **62**, 1851-1863.
29. R. D. Shannon and C. T. Prewitt, *Acta Crystallographica Section B Structural Crystallography and Crystal Chemistry* 1969, **25**, 925-946.
30. Y. S. Han, G. Hadiko, M. Fuji and M. Takahashi, *Journal of Crystal Growth*, 2005, **276**, 541-548.
31. T. J. Reich, S. Das, C. M. Koretsky, T. J. Lund and C. J. Landry, *Chemical Geology*, 2010, **275**, 262-271.
32. R. J. Crawford, I. H. Harding and D. E. Mainwaring, *Langmuir*, 1993, **9**, 3050-3056.
33. K. Mahatantila, Y. Seik and M. Okumura, *International Journal of Engineering Science and Technology*, 2011, 1655-1666.
34. L. Z. Lakshtanov and S. L. S. Stipp, *Geochimica Et Cosmochimica Acta*, 2007, **71**, 3686-3697.
35. T. Astrup, J. J. Dijkstra, R. N. J. Comans, H. A. Van der Sloot and T. H. Christensen, *Environmental Science & Technology*, 2006, **40**, 3551-3557.
36. P. Van Herck, B. Van der Bruggen, G. Vogels and C. Vandecasteele, *Waste Management*, 2000, **20**, 203-210.
37. J. P. Andreassen, *Journal of Crystal Growth*, 2005, **274**, 256-264.
38. G. T. Zhou, J. C. Yu, X. C. Wang and L. Z. Zhang, *ChemInform*, 2004, **35**, 1027-1031
39. K. Fuchigami, Y. Taguchi and M. Tanaka, *Advanced Powder Technology*, 2009, **20**, 74-79.
40. J. M. Qian and Z. H. Jin, *Industrial minerals and processing*, 2002, **31**, 1-4.
41. O. Gines, J. M. Chimenos, A. Vizcarro, J. Formosa and J. R. Rosell, *Journal of Hazardous Materials*, 2009, **169**, 643-650.
42. J. Hyks, T. Astrup and T. H. Christensen, *Journal of Hazardous Materials*, 2009, **162**, 80-91.
43. G. Cornelis, T. Van Gerven and C. Vandecasteele, *Journal of Hazardous Materials*, 2006, **137**, 1284-1292.

Figure.1

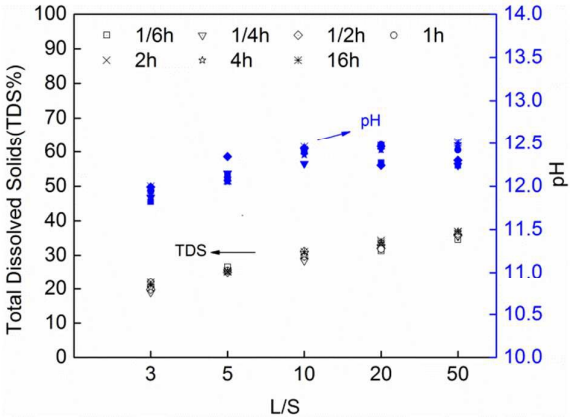

Fig. 1. TDS content (wt %) and pH of the wastewater from MSWI fly ash washing as a function of L/S ratio and washing duration. The solid symbols represent pH; the hollow symbols represent TDS.

Figure.2

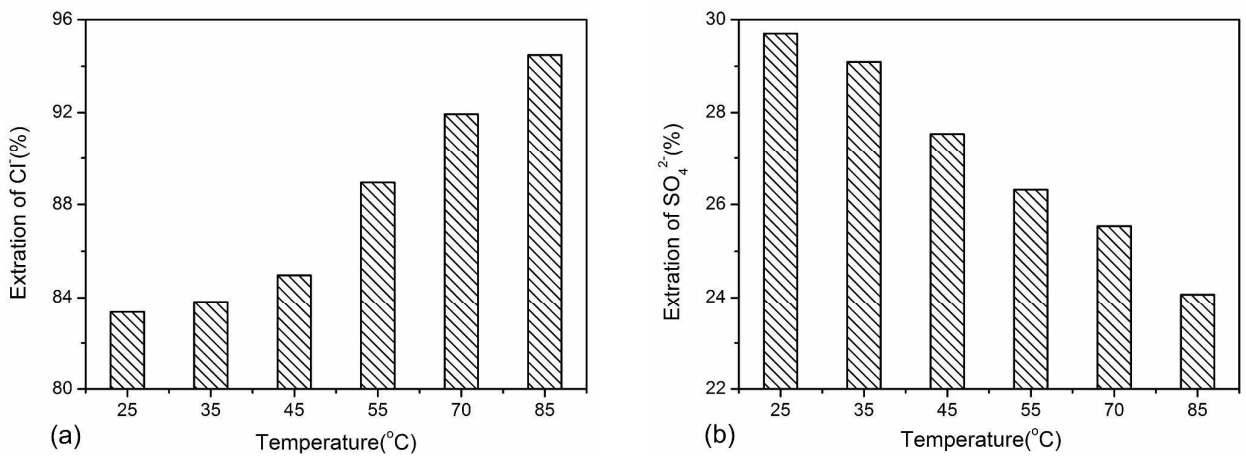

Fig. 2. Extraction of chloride and sulfate from MSWI fly ash as function of temperature

Figure.3

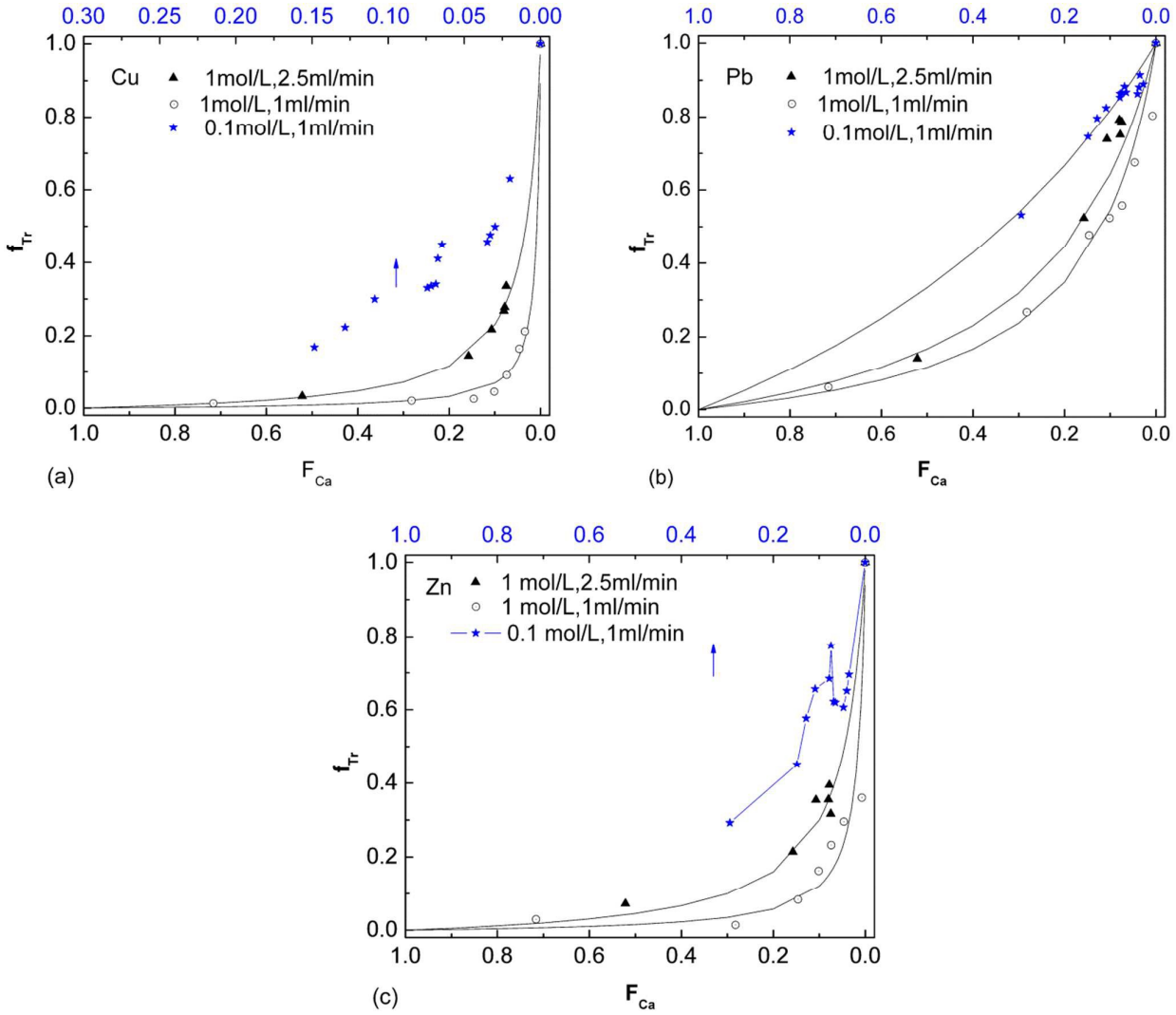

Fig. 3. Fraction of trace elements remaining in the waste wash water (f_{Tr}) after the addition of Na_2CO_3 as a function of the fraction of Ca removed (F_{Ca}). Fig. 3(a) Cu removal; Fig. 3(b) Pb removal; and Fig. 3(c) Zn removal. Initial Cu concentration ($C_{0,Cu}$) = 0.40 mg·L^{-1}; initial Pb concentration ($C_{0,Pb}$) = 63.7 mg·L^{-1}; initial Zn concentration ($C_{0,Zn}$) = 4.53 mg·L^{-1}.

Figure.4

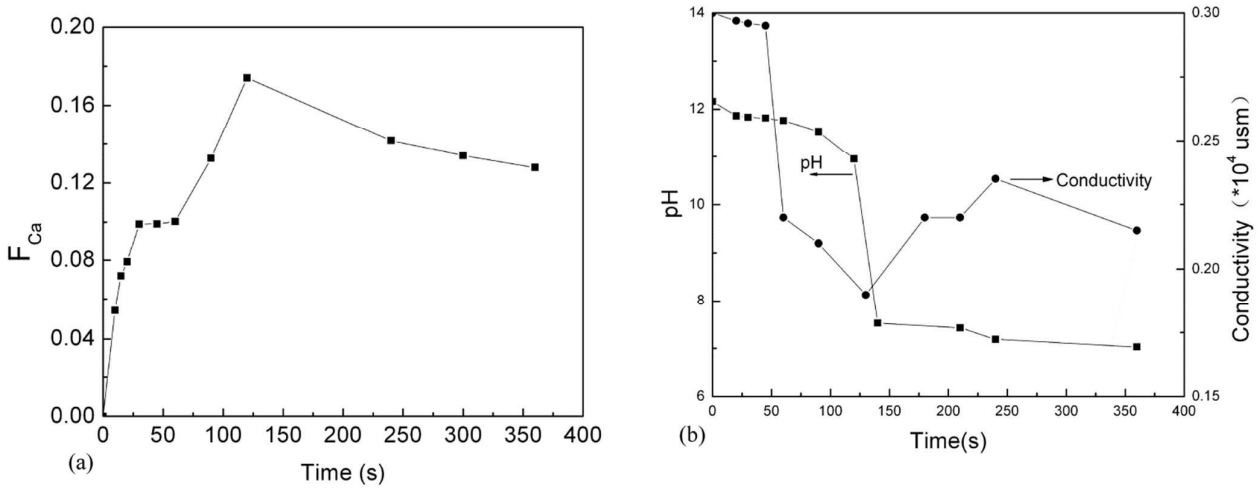

Fig. 4. Conductivity and pH in waste wash water (L/S ratio=10, washing duration=10 min) as a function of time while bubbling CO_2 into the wastewater at a flow rate of 10 mL·min^{-1}. Fig. 4(a) shows the removal ratio of Ca (F_{Ca}); Fig. 4(b) shows the pH and conductivity change. The square points represent pH, and the circular points represent conductivity.

Figure.5

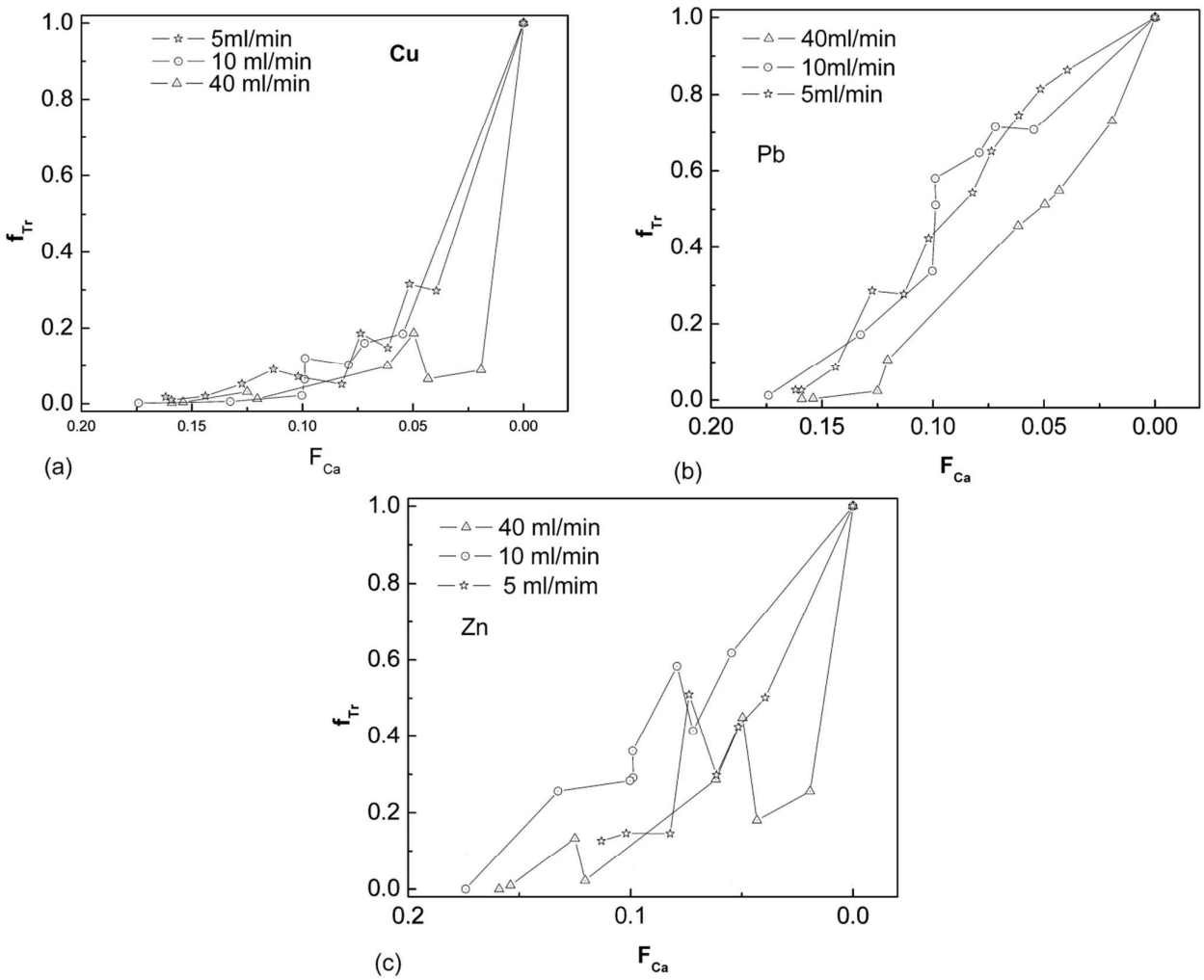

Fig. 5. Trace elements retained in the waste wash water when CO_2 was bubbled at different flow rates. In these figures, the horizontal axis is the Ca^{2+} removal ratio (F_{Ca}), while the vertical axis is the dimensionless settled fraction of trace element in the waste water (f_{Tr}, where f is the retained fraction and Tr is the trace element).

Figure.6

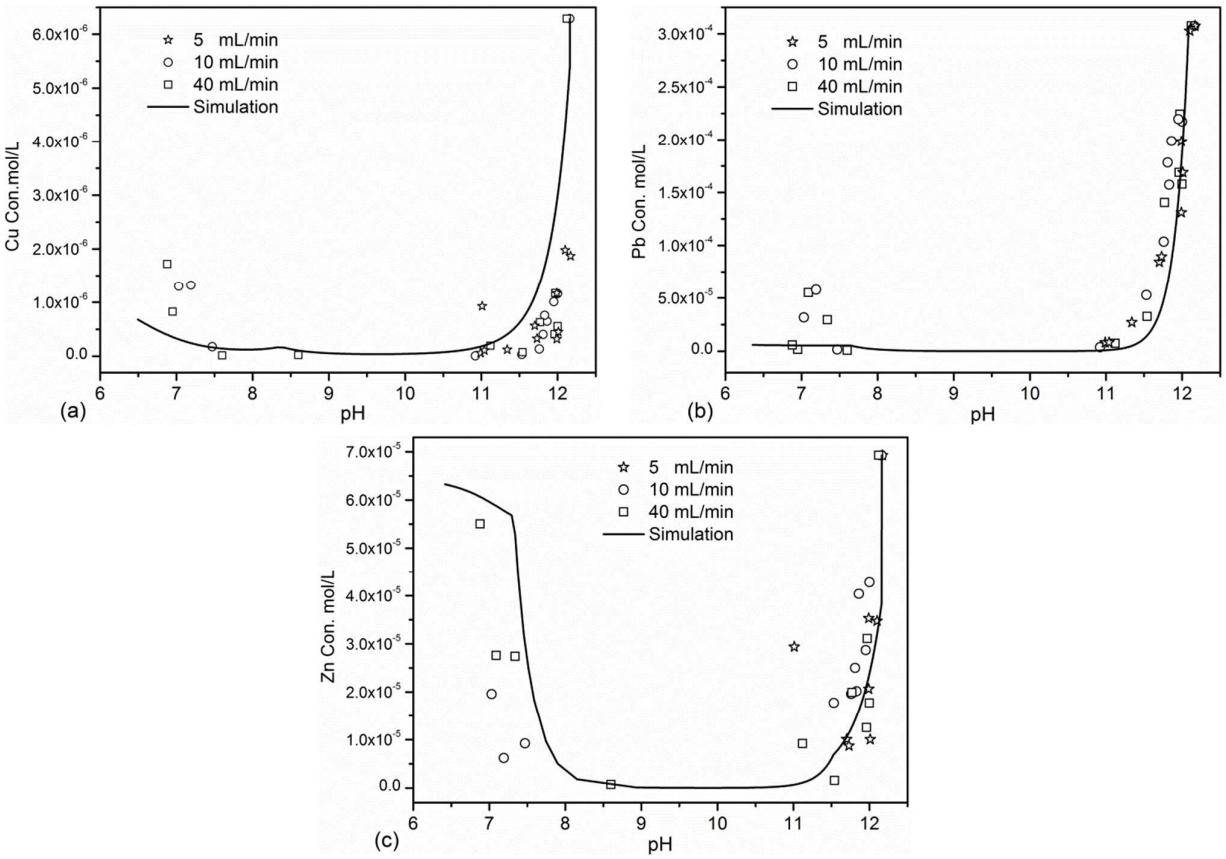

Fig. 6. Trace elements (Cu, Pb and Zn, respectively) concentration as pH changed.

Figure.7

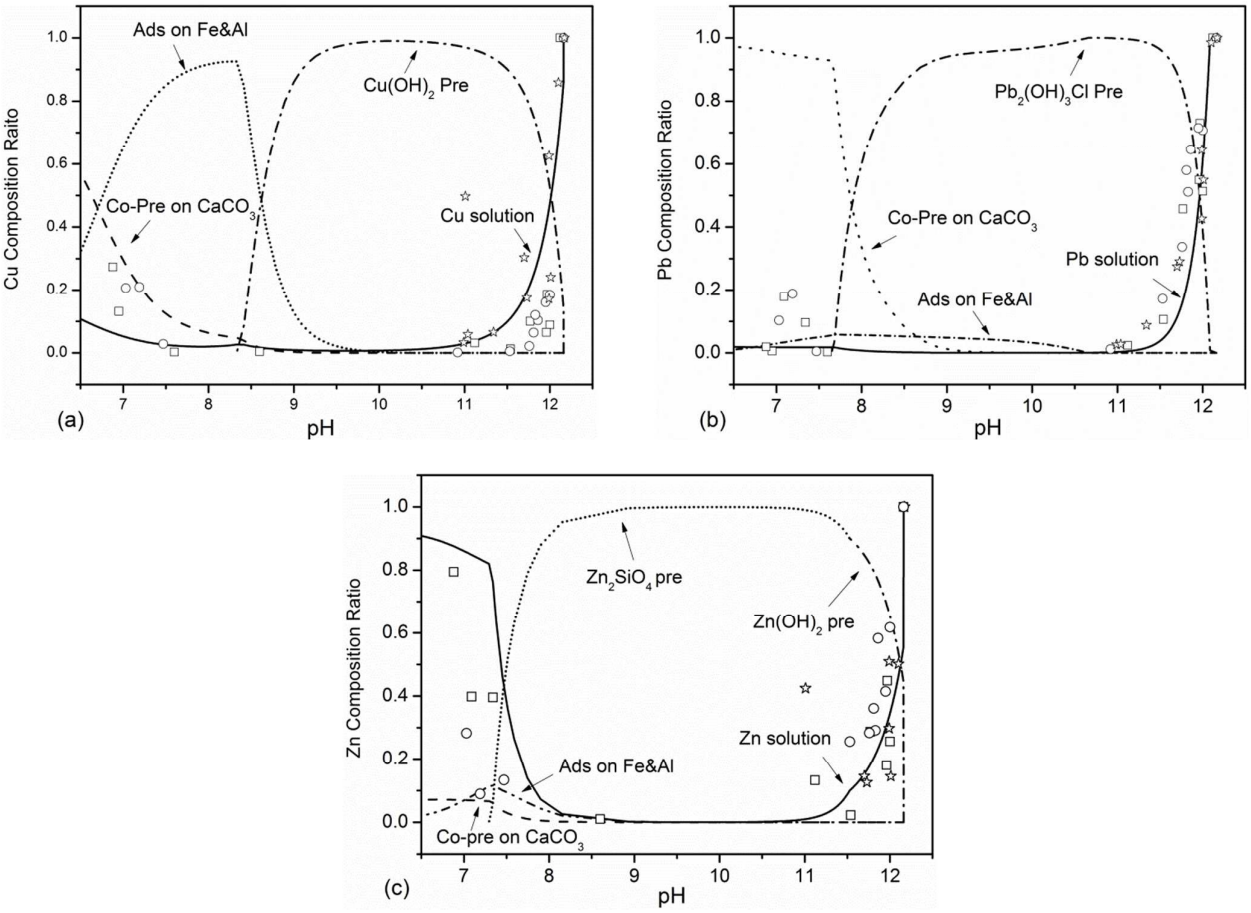

Fig. 7. The modeling results predicting the behavior of Cu, Pb and Zn, respectively. The solid line represents the solution of a trace element, and the dotted lines are the single case of a trace element. (Abbreviations used in the figure are: "pre" = precipitation and "Ads" = adsorption.)

Figure. 8

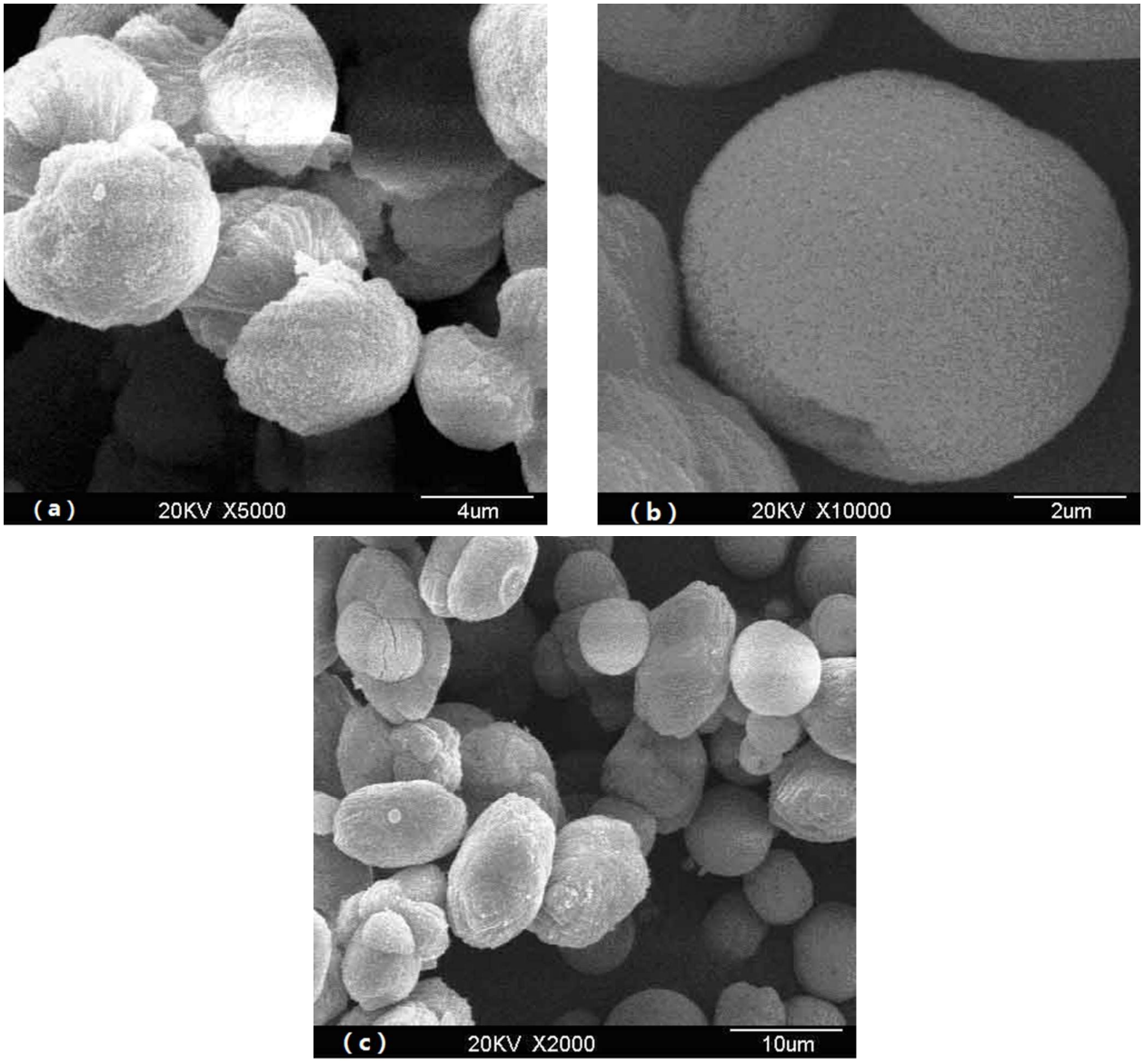

Fig. 8. Morphology of $CaCO_3$ precipitated from ash washing wastewater. The CO_2 flow rate was 40 $mL \cdot min^{-1}$.The washing duration was 10 min. Fig. 8(a) L/S = 3; Fig. 8(b) L/S = 10; Fig. 8(c) L/S = 20.

Figture .9

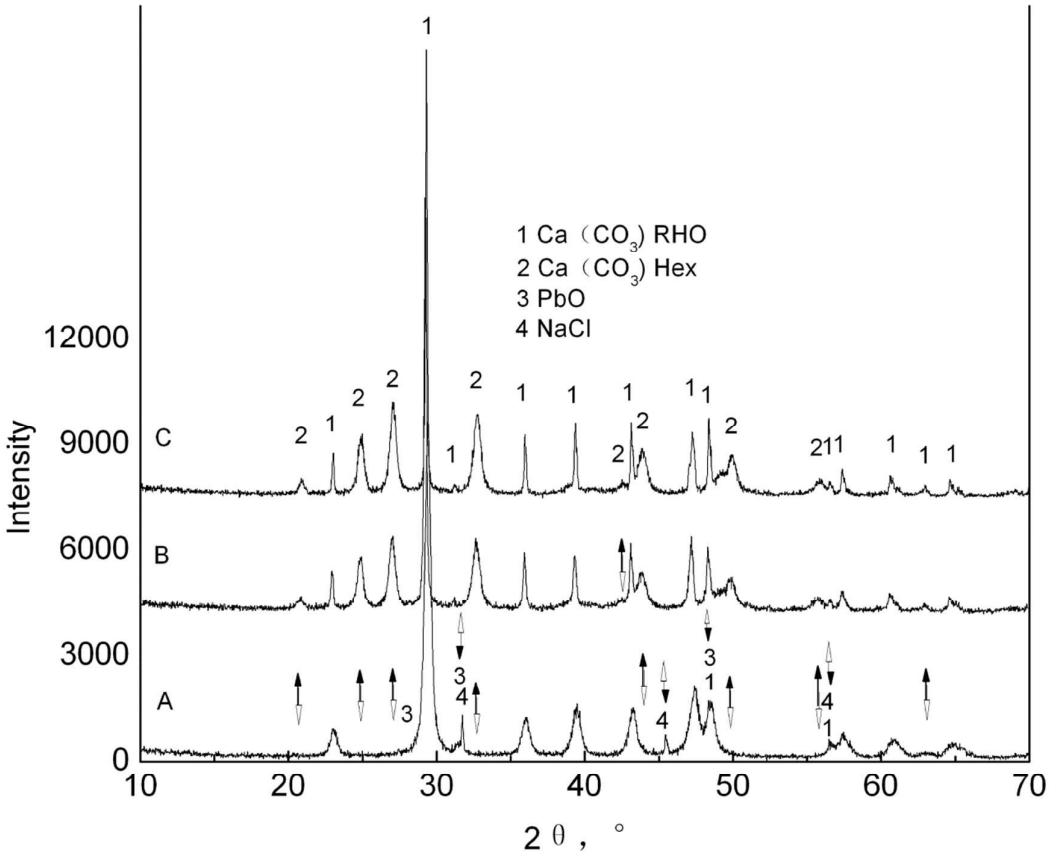

Fig. 9. XRD diffractogram of precipitation sediments from the treatment of fly ash wash water. Fig. 9(a) is the diffractogram of sediment precipitated by adding Na_2CO_3 solution to the wastewater. The washing duration was 10 min and L/S = 10. Fig. 9(b) is the diffractogram of sediment precipitated by bubbling CO_2 at a flow rate of 40 $mL \cdot min^{-1}$ into the wastewater. The washing duration was 10 min and L/S = 10. Fig. 9(c) is the diffractogram of sediments precipitated by bubbling the CO_2 at a flow rate of 40 $mL \cdot min^{-1}$ into the wastewater. The washing duration was 10 min and L/S = 3.

Figure.10

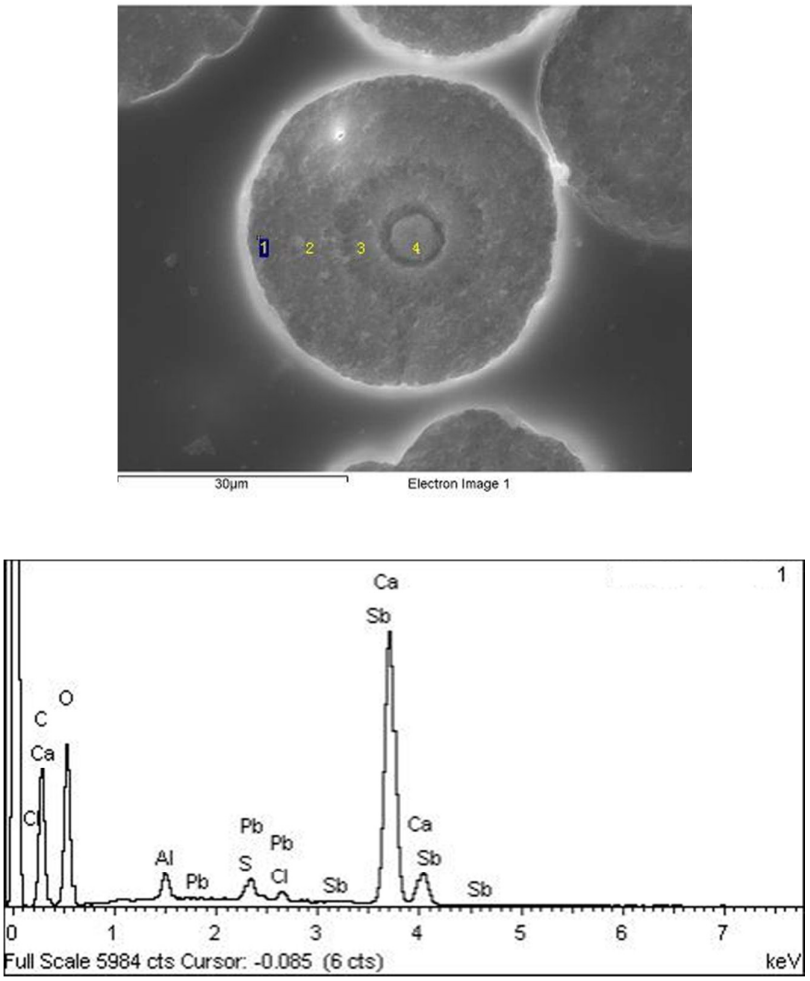

Fig. 10. SEM-EDS analysis of a typical sphere of the precipitate formed during treatment of waste fly ash wash water by CO_2 bubbling. Fig. 10(a) is a back-scattered image of the precipitate; Fig. 10(b) is the EDS analysis of the precipitate.

Table 1 Chemical composition in major and minor elements of MSWI fly ash

Item	Content %	Item	Content %
CaO	53.0	Na_2O	5.7
SiO_2	4.4	K_2O	5.5
Al_2O_3	0.9	MgO	/
Fe_2O_3	1.8	P_2O_5	0.3
TiO_2	0.6	MnO	0.1
Cl	18.9	SO_3	5.2
Minor elements	$mg \cdot kg^{-1}$	Minor elements	$mg \cdot kg^{-1}$
Zn	5279	W	22
Pb	2251	Co	21
Cu	1427	As	20
Cr	103	Mo	17
Cd	97	Zr	11
Sb	651	Ag	8
Sn	535	Nb	5
Ba	275	Bi	7
Sr	126	Hg	3
Ni	73	Ga	2

Table 2 The input data of the modeling (water=1kg)

Ion	Concentration (mmol/kgw)
Na	11.71
K	47.66
Ca	100.5
Mg	1.3×10^{-3}
Al	0.17
Fe	9.6×10^{-3}
Mn	3.3×10^{-4}
Cl	443.91
SO_4	1.61
Cd	2.7×10^{-5}
Zn	6.9×10^{-2}
Pb	0.31
Cu	6.5×10^{-3}

Table 3 Solution species used to define association reaction for aqueous species

Formula	log_k
$Ca^{2+} + H_2O = CaOH^+ + H^+$	-12.780
$Ca^{2+} + CO_3^{2-} + H^+ = CaHCO_3^+$	11.599
$Ca^{2+} + CO_3^{2-} = CaCO_3$	3.224
$Cu^{2+} + H_2O = CuOH^+ + H^+$	-7.497
$Cu^{2+} + 2H_2O = Cu(OH)_2 + 2H^+$	-16.194
$Cu^{2+} + 3H_2O = Cu(OH)_3^- + 3H^+$	-27.8
$Cu^{2+} + 4H_2O = Cu(OH)_4^{2-} + 4H^+$	-39.6
$Cu^{2+} + CO_3^{2-} = CuCO_3$	6.77
$2CO_3^{2-} + Cu^{2+} = Cu(CO_3)_2^{2-}$	9.83
$2Pb^{2+} + H_2O = Pb_2OH^{3+} + H^+$	-6.3951
$3H_2O + Pb^{2+} = Pb(OH)_3^- + 3H^+$	-27.2
$2H_2O + Pb^{2+} = Pb(OH)_2 + 2H^+$	-16.95
$Pb^{2+} + 4H_2O = Pb(OH)_4^{-2} + 4H^+$	-38.9
$4Pb^{2+} + 4H_2O = Pb_4(OH)_4^{4+} + 4H^+$	-20.8803
$4H_2O + 3Pb^{2+} = Pb_3(OH)_4^{2+} + 4H^+$	-23.88
$CO_3^{2-} + Pb^{2+} = PbCO_3$	7.24
$2CO_3^{2-} + Pb^{2+} = Pb(CO_3)_2^{2-}$	10.64
$HCO_3^- + Pb^{2+} = PbHCO_3^+$	2.9
$H_2O + Zn^{2+} = ZnOH^+ + H^+$	-8.96
$2H_2O + Zn^{2+} = Zn(OH)_2 + 2H^+$	-17.794
$3H_2O + Zn^{2+} = Zn(OH)_3^- + 3H^+$	-28.4
$4H_2O + Zn^{2+} = Zn(OH)_4^{2-} + 4H^+$	-41.2
$CO_3^{2-} + Zn^{2+} = ZnCO_3$	5.3
$2CO_3^{2-} + Zn^{2+} = Zn(CO_3)_2^{2-}$	9.63
$HCO_3^- + Zn^{2+} = ZnHCO_3^+$	2.1

Table 4 Phase used to define mineral

Item	Formula	log_k
Gibbsite	$Al(OH)_3 + 3H^+ = Al^{3+} + 3H_2O$	8.11
Goethite	$FeOOH + 3H^+ = Fe^{3+} + 2H_2O$	-1
Portlandite	$Ca(OH)_2 + 2H^+ = Ca^{2+} + 2H_2O$	22.804
Calcite	$CaCO_3 = CO_3^{2-} + Ca^{2+}$	-8.480
Anhydrite	$CaSO_4 = Ca^{2+} + SO_4^{2-}$	-4.360
$Cu(OH)_2$(s)	$Cu(OH)_2 + 2H^+ = Cu^{2+} + 2H_2O$	8.674
$CuCO_3$	$CuCO_3 = Cu^{2+} + CO_3^{2-}$	-11.5
Malachite	$Cu_2(OH)_2CO_3 + 2H^+ = 2Cu^{2+} + 2H_2O + CO_3^{2-}$	-5.306
Cerrusite	$PbCO_3 = CO_3^{2-} + Pb^{2+}$	-13.13
$Pb_2(OH)_3Cl$	$Pb_2(OH)_3Cl + 3H^+ = 2Pb^{2+} + 3H_2O + Cl^-$	8.793
$Zn(OH)_2$	$Zn(OH)_2 + 2H^+ = 2H_2O + Zn^{2+}$	11.5
Smithsonite	$ZnCO_3 = CO_3^{2-} + Zn^{2+}$	-10

Table 5 Orthogonal experimental design and the results

No.	L/S Ratio	Washing duration	Extration of Cl^-(%)	Extration of SO_4(%)
1	3	5	58.5	12.5
2	3	10	63.7	12.7
3	3	30	61.1	13.3
4	3	60	63.9	14.2
5	5	10	82.8	25.6
6	5	30	83.2	25.1
7	5	60	84.1	26.3
8	5	5	79.2	27.0
9	10	30	85.4	31.0
10	10	60	84.1	31.0
11	10	5	83.5	29.3
12	10	10	83.4	29.8
13	20	60	85.1	38.2
14	20	10	85.4	34.4
15	20	30	81.2	37.9
16	20	5	84.7	31.4

Table 6 Parameters of orthogonal experiment

Parameters	Extration of Cl^-		Extration of SO_4^{2-}	
	L/S Ratio	Washing duration	L/S Ratio	Washing duration
I_1	247.2	305.9	52.6	100.2
I_2	329.2	315.2	104.0	102.4
I_3	336.34	310.8	121.1	107.3
I_4	336.28	317.2	141.8	109.7
K_1	61.8	76.5	13.2	25.1
K_2	82.3	78.8	26.0	25.6
K_3	84.09	77.7	30.3	26.8
K_4	84.07	79.3	35.5	27.4
R	22.3	2.8	22.3	2.4

Table 7 Surface species used for association reaction in solution mode

formula	log_k
$Fe_s\text{-}OH + Cu^{2+} = Fe_s\text{-}OCu^{+} + H^{+}$	2.89
$Fe_w\text{-}OH + Cu^{2+} = Fe_w\text{-}OCu^{+} + H^{+}$	0.6
$Al_s\text{-}OH + Cu^{2+} = Al_s\text{-}OCu^{+} + H^{+}$	2.89
$Al_w\text{-}OH + Cu^{2+} = Al_w\text{-}OCu^{+} + H^{+}$	0.6
$Fe_s\text{-}OH + Pb^{2+} = Fe_s\text{-}OPb^{+} + H^{+}$	4.65
$Fe_w\text{-}OH + Pb^{2+} = Fe_w\text{-}OPb^{+} + H^{+}$	0.3
$Al_s\text{-}OH + Pb^{2+} = Al_s\text{-}OPb^{+} + H^{+}$	4.65
$Al_w\text{-}OH + Pb^{2+} = Al_w\text{-}OPb^{+} + H^{+}$	0.3
$Fe_s\text{-}OH + Zn^{2+} = Fe_s\text{-}OZn^{+} + H^{+}$	0.99
$Fe_w\text{-}OH + Zn^{2+} = Fe_w\text{-}OZn^{+} + H^{+}$	-1.99
$Al_s\text{-}OH + Zn^{2+} = Al_s\text{-}OZn^{+} + H^{+}$	0.99
$Al_w\text{-}OH + Zn^{2+} = Al_w\text{-}OZn^{+} + H^{+}$	-1.99

Table 8 Corresponding minimum concentration of trace elements in wastewater after CO_2 bubbling $mg \cdot L^{-1}$

Trace element	Initial concentration	Final concentration after CO_2 bubbling with the flow rate of			Discharge limits
		40 $ml \cdot min^{-1}$	10 $ml \cdot min^{-1}$	5 $ml \cdot min^{-1}$	
Pb	63.70	0.128	0.519	1.123	0.1
Zn	4.53	0.026	0.046	0.570	0.1
Cu	0.40	0.001	$0.54*10^{-3}$	0.007	0.01

Table 9 Chemical composition of the precipitates %

	C	O	Al	S	Cl	Ca	Sb	Pb	Total
1	**20.33**	43.49	1.27	1.17	0.75	**29.88**	2.03	**1.08**	100
2	**9.96**	46.91	2.01	1.38		**37.65**	0.83	**1.25**	100
3	**9.11**	42.34	0.85	1.33		**42.64**	2.46	**1.27**	100
4	**5.25**	32.16	0.52	1.56		**55.96**	3.20	**1.35**	100

Graphical Abstract

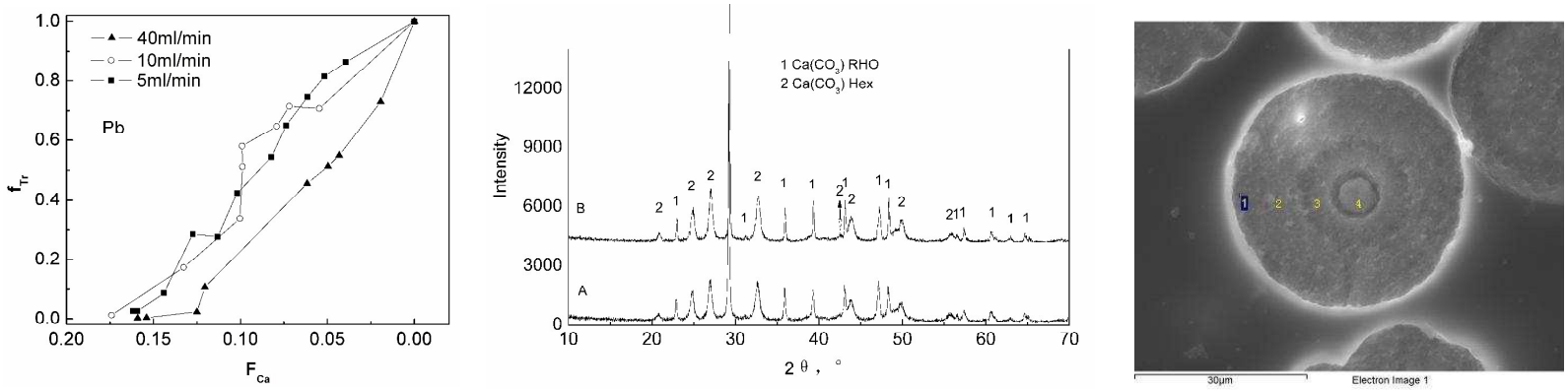

Co-precipitation of Pb with Fe and Al colloid and $CaCO_3$ when CO_2 is bubbled into the solution of MSWI fly ash water washing effluent, whose character is high pH value, high Ca^{2+} content and high amphoteric heavy metal concentrations. The major precipitation product is $CaCO_3$.The concentration of Pb in the product is different along the radius direction. L. Wang *, G.C. Xing, I.A. Jamro, Q. Chen, L.H. Wei, H.A Baloch